To appear in "Building Galaxies: From the Primordial Universe to the Present," Proceedings of the XIXth Moriond Astrophysics Meeting, eds. F. Hammer et al., 1999.

SIRTF Studies of Galaxy Formation and Evolution

P. Eisenhardt
Jet Propulsion Laboratory, California Institute of Technology, Pasadena, USA

Abstract

The Space Infrared Telescope Facility (*SIRTF*) is a cornerstone of NASA's Origins program, and will complete NASA's family of Great Observatories when it is launched in December 2001. *SIRTF* will provide imaging with point source sensitivities ranging from a few μJy at 3.6μm to $\sim$ 20 mJy at 160μm, and spectroscopy of sources brighter than a mJy over the $5 - 40\mu$m range. Over 75% of observing time during *SIRTF*'s expected 5 year lifetime will be available to general investigators from the international community, with the first call for proposals in July 2000. I review *SIRTF*'s capabilities and plans for the study of galaxy formation and evolution.

1 Introduction

After many years of conceptual design studies, the *Space Infrared Telescope Facility* (*SIRTF* - Figure 1) has entered its final construction phase [4]. *SIRTF* will consist of a 0.85-meter cryogenically-cooled telescope and three science instruments capable of performing imaging and spectroscopy in the $3 - 180\mu$m wavelength band. With launch planned for December 2001, *SIRTF* will complete NASA's family of Great Observatories. Large format infrared detector arrays, coupled with innovative choices in orbit and system architecture will give *SIRTF* a large increase in sensitivity across its wavelength range, compared to previous missions such as *IRAS* and *ISO*. Over 75% of the observing time during its 2.5 year-minimum (5 year goal) lifetime will be awarded to general investigators. A call for Legacy Proposals (large projects of both immediate scientific interest and lasting archival value, and with no proprietary data period) is planned for July of 2000. For the most up-to-date information on *SIRTF*, see http://sirtf.caltech.edu.

2 Infrared Observations and Galaxy Formation

Studies of galaxy formation and evolution have been one of the chief motivations for *SIRTF* since its inception. There are several fundamental reasons why infrared observations are crucial for such studies. These include the cosmological redshift, the ubiquity of the H^- ion as a dominant opacity source in stellar populations, and the importance of dust in modulating the spectral energy distribution of star forming regions.

It is almost a tautology to state that infrared data are necessary to understand evolutionary effects in high redshift galaxies. Comparisons of galaxies at different lookback time must be

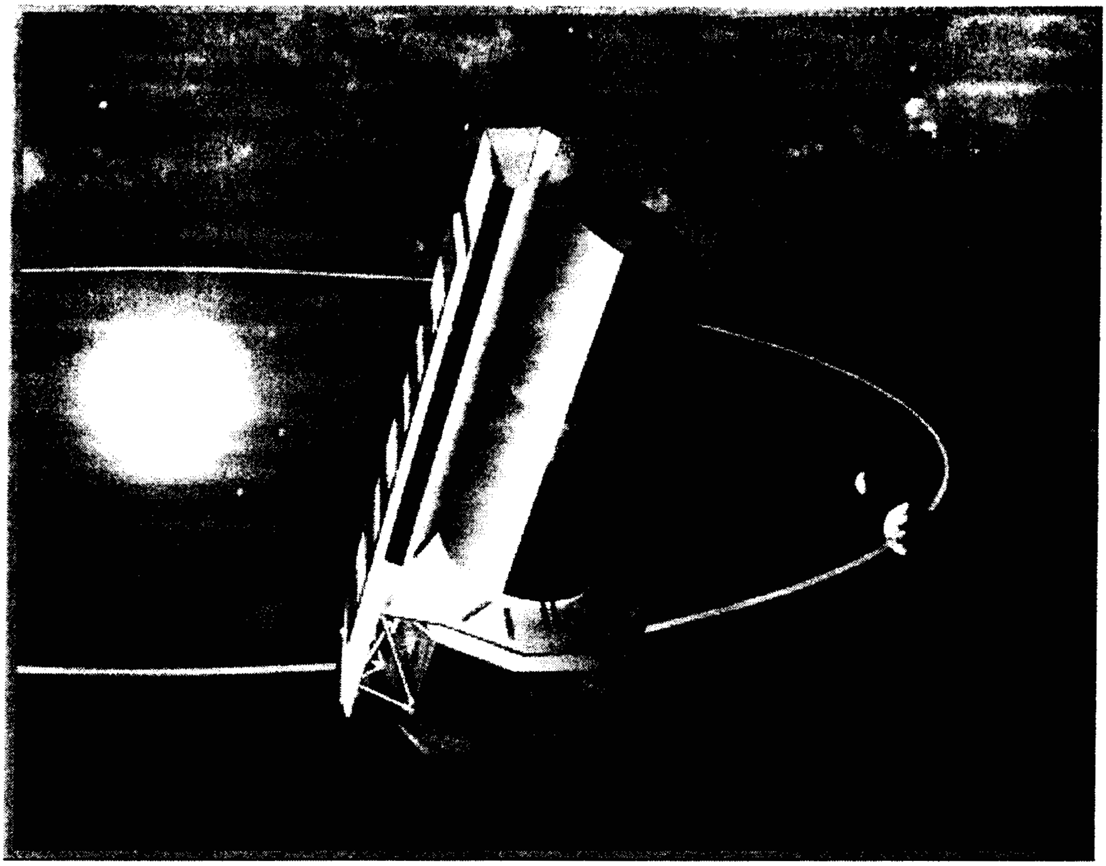

Figure 1: *SIRTF* seen in its Earth-trailing solar orbit.

made at constant rest frame wavelengths to be meaningful. For starlight the most relevant wavelengths are from the Lyman break at 912Å to the CO absorption bands at 2.3μm.

The Lyman break technique has now been extended to the point ($z \gtrsim 7$) that galaxies at the high redshift frontier are undetectable without infrared observations [15], [2]. The Lyman break technique samples rest frame UV light emitted by the hottest stars and hence is an excellent guide to unobscured star-forming populations. Extending this technique to even higher redshifts is likely to require *NGST*.

But the spectra of the garden variety stars and galaxies we know most about peak in the near infrared, because of the H^- opacity minimum at 1.6μm [13]. Identifying large samples of high redshift galaxies in the rest frame near IR has been one of the defining scientific programs for *SIRTF* for many years.

Finally, star formation, at least locally, is strongly associated with dust and hence with high levels of UV extinction. Meurer, Heckman, & Calzetti [17] and Steidel et al. [25] have used the correlation of UV spectral index with far IR emission to estimate that extinction corrections to estimates of the global star formation rate are a factor of 5. Recent far-infrared detections of the cosmic background [8], and far-infrared and submillimeter detections of field galaxies with *ISO* and SCUBA [14], [18], [1], [12] also hint at a heavily dust enshrouded starburst population in the early universe. Whether these sources are in fact starbursts or are powered by AGN, what their bolometric luminosities are, and what their redshift distribution is, are very much open questions. Again, the identification and characterization of distant ultra-luminous infrared galaxies (ULIRG's) has been used to help define *SIRTF*'s functionality.

constraints imposed by the Earth, providing much simpler operations than are possible in an Earth orbit. *SIRTF*'s window of visibility on the celestial sky will form an annulus, perpendicular to the ecliptic plane, with allowed solar elongations ranging from 80 to 120 degrees. All regions of the sky will be visible to *SIRTF* twice a year, for a minimum of ≈ 40 days each period (at the ecliptic equator). The visibility periods increase to $\gtrsim 200$ days per year at an ecliptic latitude of 60°, and constant viewing is possible within 10°of the ecliptic poles. About a third of the sky will be instantaneously visible to *SIRTF* at any given time.

4 *SIRTF* Instruments

The *SIRTF* instruments are the Infrared Array Camera (IRAC - G. Fazio, SAO, PI [5]); the Infrared Spectrograph (IRS - J. Houck, Cornell, PI [20]); and the Multiband Imaging Photometer for *SIRTF* (MIPS - G. Rieke, U. Arizona, PI [11]). In addition, Pointing Calibration Reference Sensor (PCRS) arrays are used to facilitate precision pointing of the instruments (Figure 2).

IRAC provides imaging at 3.6, 4.5, 5.8, and 8μm, with predicted point source sensitivities (5σ in 500 sec) of ≈ 3, 4, 10, and 15μJy respectively. All bands use arrays with 256^2 $1''.2$ pixels, with InSb detectors for the two shorter wavelengths, and Si:As IBC detectors for the two longer longer wavelengths. Dichroic beamsplitters allow the 3.6 and 5.8μm arrays to view the same $5'.1 \times 5'.1$ field while an adjacent field is simultaneously imaged at 4.5 and 8μm. A shutter allows dark current and absolute sky brightness measurements, and its mirrored inner surface can also be illuminated by calibration sources.

The IRS uses a 128^2 pixel Si:As IBC array and a 128^2 pixel Si:Sb IBC array to provide low resolution (R ≈ 50) long-slit ($1' - 2'.5$) spectroscopy from $5 - 40\mu$m. A second pair of these arrays provides moderate resolution (R ≈ 600) echelle spectroscopy with $12'' - 22''$ slits from $10 - 40\mu$m. The low resolution sensitivity is ~ 1 mJy (5σ in 500 sec), while the line sensitivity in the echelle mode is $\approx 3 \times 10^{-18}$ W/m^2. Part of the low resolution Si:As array is used to obtain "peak-up" images over two $1' \times 1'.2$ fields: one covering $13 - 18\mu$m, the other $18 - 26\mu$m. Onboard centroids are determined from these peak-up images to offset the source directly onto the selected slit with sub-arcsecond accuracy.

The MIPS provides imaging over a $5'.3$ field using a 128^2 pixel Si:As IBC array at 24μm, and a 32^2 pixel Ge:Ga photoconductor array at 100μm. A 2×20 pixel stressed Ge:Ga photoconductor array images a $0'.5 \times 5'.3$ field at 160μm. Predicted 5σ in 500 second sensitivities are 0.37, 1.4, and 22.5 mJy respectively in the three bands (the 160μm value is limited by confusion). A scan mirror derived from the design proven in *ISO*'s SWS instrument allows sources to be chopped on and off the detectors. The scan mirror also enables MIPS to efficiently survey large areas, by freezing an image of the sky on the three detectors for several seconds while the observatory continuously scans in the opposite direction at a constant rate. Other settings of the scan mirror enable a fully-sampled, higher magnification mode at 70μm, and an R ≈ 15 spectral energy distribution mode from $52 - 99\mu$m.

5 *SIRTF* and Galaxy Formation and Evolution

Relative to *ISO*, *SIRTF*'s detector arrays provide typically $1 - 2$ orders of magnitude better sensitivity, coupled with $1 - 2$ orders of magnitude more pixels. These gains are sufficient to bring vast numbers of distant galaxies at large lookback times within *SIRTF*'s grasp.

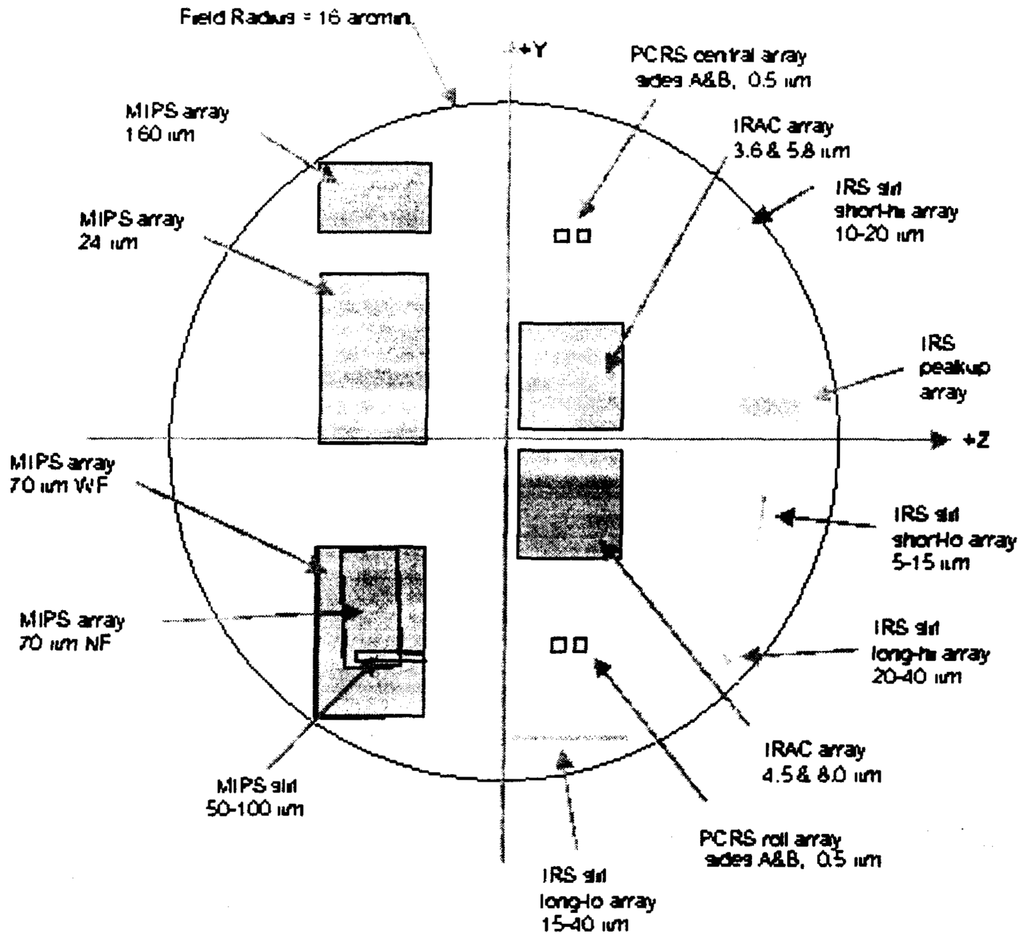

Figure 2: Approximate locations of *SIRTF* instrument apertures projected onto the sky. A scan mirror enables the MIPS arrays to cover the rectangular regions shown; the instantaneous fields are actually $5'.3$ square at 24 and 70μm and $0'.5 \times 5'.3$ at 160μm.

3 *SIRTF* Mission Overview

The Observatory is shown in Figure 1. Several innovative design features have enabled *SIRTF* to retain the majority of the originally envisioned science capability at a fraction of the original cost and mass.

SIRTF's 85-cm aperture Cassegrain telescope is cooled by helium vapor to 5.5 K. The telescope primary and secondary mirrors are constructed of beryllium, and the f-ratio of the system is f/12. The telescope is a Ritchey-Chretien design, diffraction limited at a wavelength of 6.5μm. Three science instruments share the 32 arcminute diameter focal plane (Figure 2), and are located in a chamber cooled to 1.4 K by superfluid helium. A major technical development of the *SIRTF* mission has been the implementation of a "warm-launch architecture," in which *SIRTF*'s telescope assembly is launched at ambient temperature and allowed to cool radiatively (passively) to $\approx$ 30K, and only then thermally connected to the helium tank. Only the focal-plane instruments and the compact liquid helium cryostat are enclosed in a vacuum shell. This has led to a dramatic reduction in the volume of liquid cryogen required (360 liters) for the 5-year mission.

A Delta 7920-H rocket will be used to launch *SIRTF* directly into an Earth-trailing heliocentric orbit, which drifts away from the Earth at approximately 0.1 AU per year. No orbit corrections or adjustments are envisaged. This orbit removes the thermal load and viewing

5.1 Redshifted Starlight

One of the defining scientific programs for *SIRTF* is the study of galaxies to $z > 3$ by means of deep surveys at $3 - 10\mu m$. This limit was selected because it is apparently beyond the peak in the space density of luminous quasars [22]. Not only will IRAC's excellent sensitivity in this wavelength region allow such galaxies to be detected (Figure 3), but the H^- opacity minimum at $1.6\mu m$ [13] is expected to be a major tool in photometric redshift determination at $1 < z < 5$ [27], [23], since it is a ubiquitous feature of stellar atmospheres.

UV-bright examples of such galaxies have already been detected by means of the Lyman break technique [24], [25] and they play an important role in the overall star formation history of the Universe [16]. By detecting galaxies on the strength of their UV emission, however, LBG samples are necessarily biased in favor of those with both active star formation and relatively modest extinction. Such samples will not reveal if there is an underlying population of galaxies which have already assembled the bulk of their stellar mass. In the absence of ongoing star formation, even massive galaxies will be too faint in the rest-frame ultraviolet to be picked up by optical surveys. The stellar mass already present at an early epoch constrains the star formation rate to that point, a quantity which is still uncertain due to the possibility of significant dust extinction. Hence an accurate picture of the star formation history of the universe can only be determined by making an accurate census of *all* galaxies, not just star-forming ones with low extinction. Since the luminosity in the rest-frame near-infrared correlates linearly with mass [7] and is relatively unaffected by dust obscuration, this is clearly the spectral region in which to make such a census.

Figure 3 shows that IRAC sensitivity is sufficient to sample around the rest frame $1.6\mu m$ peak to $z > 3$. Scaling from existing K' selected samples, Simpson & Eisenhardt [23] estimate that IRAC could generate a sample containing roughly one thousand $z = 3L^*$ galaxies in 100 hours of observation. Beyond generating a sample selected primarily on mass, IRAC sampling of the $1.6\mu m$ peak can be used to obtain photometric redshifts. The 5.8 and $8\mu m$ IRAC filters were optimized for photometric redshifts of $z \approx 3$ galaxies [23].

As an illustration of how photometric redshifts can be derived from IRAC data, Figure 4 shows a $3.6 - 4.5\mu m$ vs. $5.6 - 8.0\mu m$ color-color plot for the galaxy models considered in Simpson & Eisenhardt [23] in the redshift range $1 < z < 5$. It can be seen that the color in the two Si:As filters is generally able to provide an excellent measurement of the galaxy redshift for $z \gtrsim 2$. For $1 \lesssim z \lesssim 2$, the $3.6 - 4.5\mu m$ color provides most of the photometric redshift signal. Only Model D has a very limited range of colors which might hamper analysis, since we are observing the Rayleigh–Jeans tail of a recent starburst with only weak metal line blanketing; however, this is exactly the sort of UV-bright galaxy which would be detected in surveys for UV dropouts, and so this does not pose a problem.

5.2 Infrared Luminous Galaxies

In the local universe, 30% or more of the bolometric energy of galaxies is emitted at $> 10\mu m$ [9], [21]. The ratio of IR to UV/optical luminosity increases with star formation rate and luminosity, and can exceed 100:1 in extreme cases. As derived from UV luminosity, both the incidence of high SFR galaxies and the global SFR were much higher at $z \gtrsim 1$ than today [16]. Hence it is plausible to expect that ultra-luminous IR starburst galaxies such as Arp 220 were also much more common at high redshift.

The detection of the cosmic infrared background (CIB) at 140 and $240\mu m$ by DIRBE [8] demonstrates that at least half of the bolometric energy integrated over the age of the Universe is found in the IR-submm range [3]. Deep observations with SCUBA reveal a population of

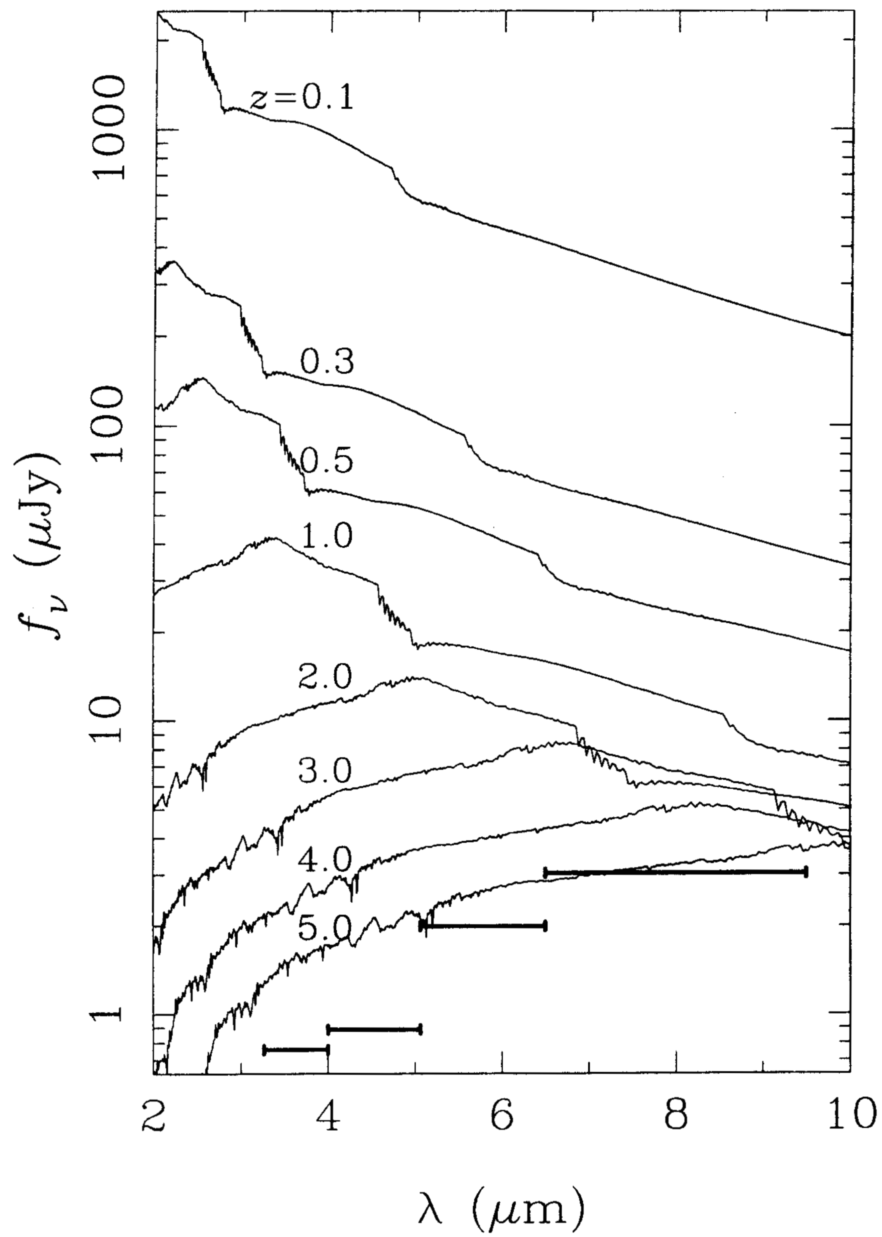

Figure 3: Model spectra as a function of redshift for a maximally old L^* galaxy in which all stars formed in an instantaneous burst at $z = \infty$, and evolve passively thereafter, in an $H_o = 50, q_o = 0.1$ cosmology. The flux is normalized to $M_K = -25.1$ today [6]. Also shown are the IRAC sensitivities (1σ in 500 seconds).

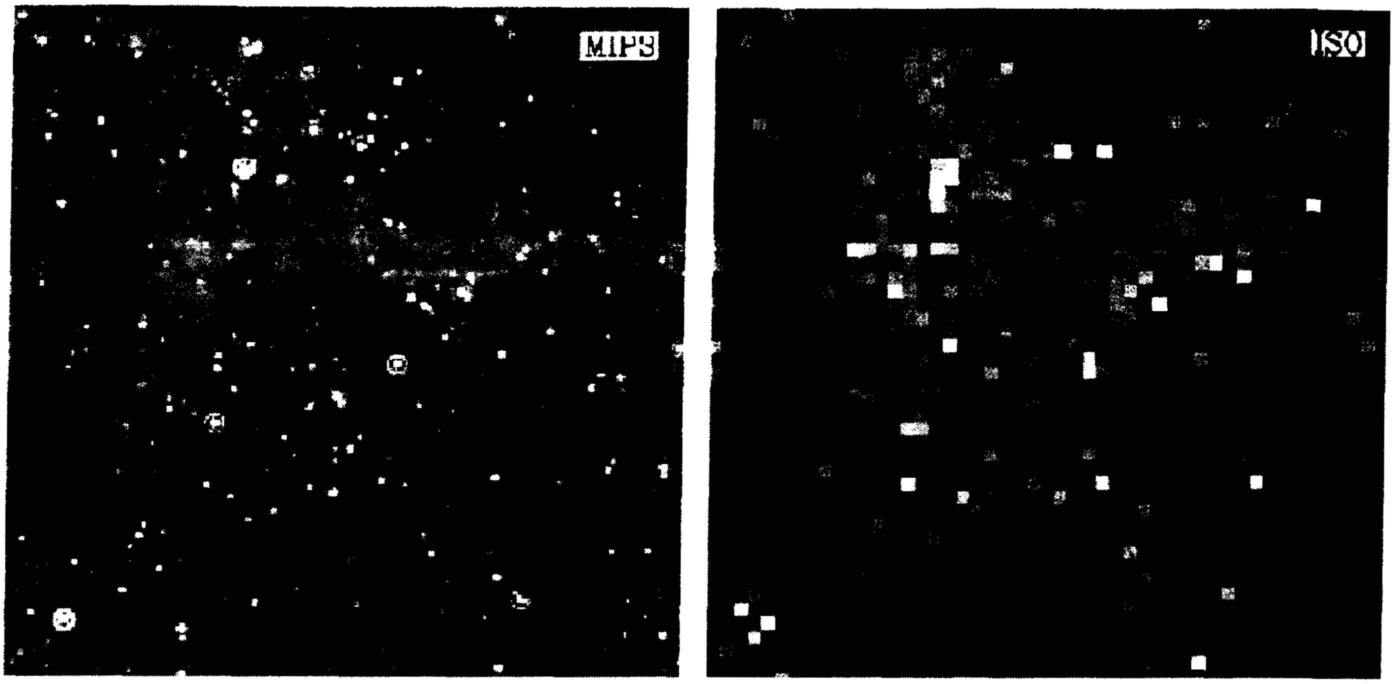

Figure 5: Simulated 70μm map of 35×35' region with MIPS (left) vs. ISO (right).

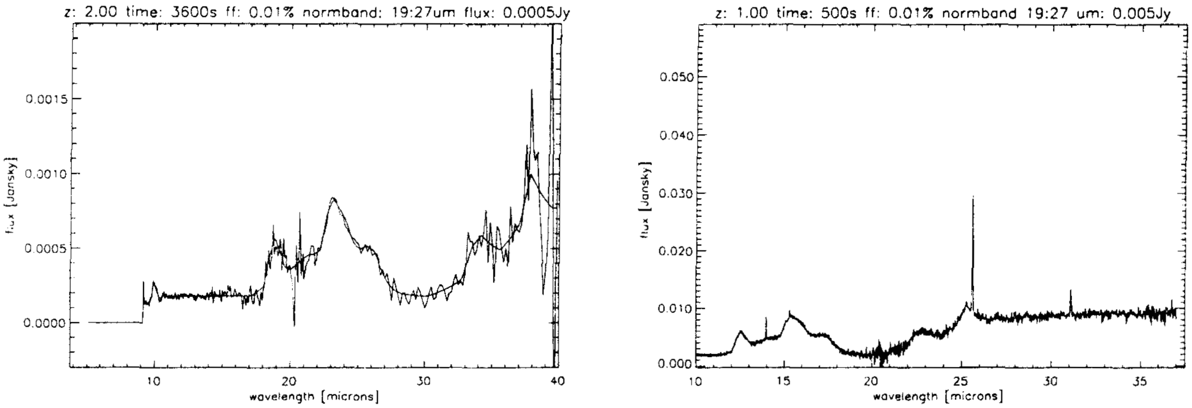

Figure 6: Simulated low-resolution IRS spectrum of an ultraluminous IR galaxy at $z = 2$ (left), and high-resolution spectrum at $z = 1$ (right).

spectrum is the rest-frame 7.7μm PAH feature. *ISO* observations have established that the strength of this feature provides good discrimination between the AGN and starburst mechanisms [10]. More luminous systems tend to have a higher incidence of AGN (and weak or non-existent 7.7μm PAH emission).

More quantitative information about excitation conditions and abundances can be obtained by measuring the strengths of the gas-phase emission lines visible in the high resolution spectrum in Figure 6. In particular ratios of the forbidden neon lines including [NeII] 12.8μm, [NeV] 14.3μm, and [NeIII] 15.6μm can readily distinguish starbursts, shocks, and AGN, and are very insensitive to extinction [26]. The high ratio of [NeII]/[NeIII] and [NeIII]/[NeV] in Figure 6 is clear evidence for a starburst.

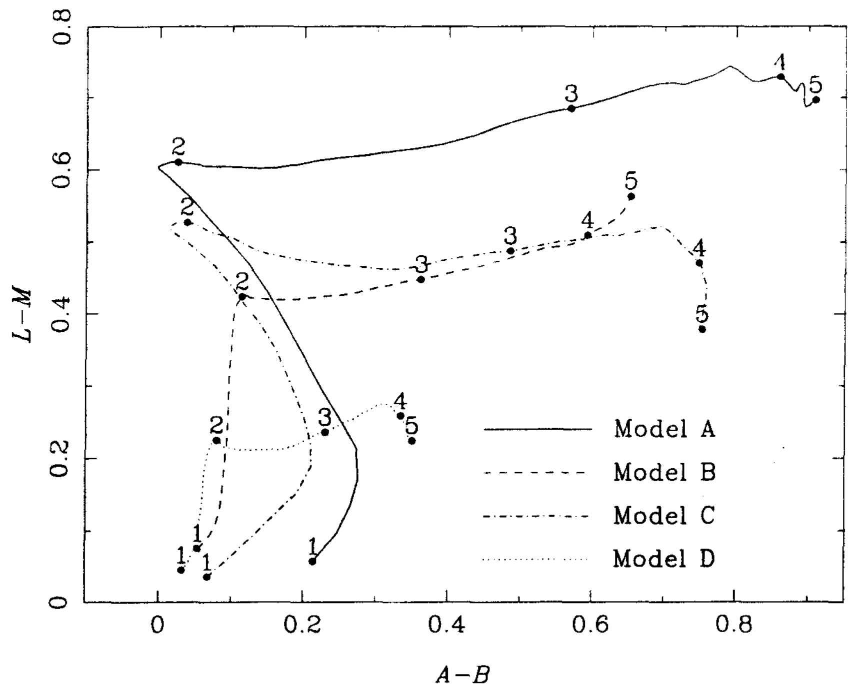

Figure 4: Loci of the four galaxy models discussed in [23] in the $L-M$ *vs* $A_p - B_p$ ($3.6-4.5\mu$m vs. $5.6-8.0\mu$m) color-color diagram. The locations of the models at z = 1,2,3,4,5 are indicated.

850μm sources with fluxes > 1 mJy which can account for much of the CIB [12], [1], while *ISO* surveys to 100 mJy at 175μm reveal a population which accounts for roughly 10% of the CIB [19].

MIPS can obtain photometry for sources similar to Arp 220 to $z \sim 2$, and should be able to identify the bulk of the discrete sources comprising the CIB at 160μm. Targeted MIPS observations of luminous LBG galaxies on the one hand, and of SCUBA sources on the other will allow the construction of complete spectral energy distributions for these objects, and show whether there is any significant overlap between objects which contribute to the UV/optical cosmic background and those which make up the CIB.

The MIPS scan mirror enables large areas to be surveyed efficiently. Figure 5 illustrates the type of data expected from 24 hours of MIPS observation, as compared to the same time with *ISO*. Surveys such as these will allow *SIRTF* to identify large enough samples to search for rare and perhaps presently unknown classes of objects.

5.3 Starbursts vs. AGN

While surveys can reveal previously unsuspected populations and determine global parameters, spectroscopy is necessary to understand the physical nature of the infrared luminous objects *SIRTF* will discover. For heavily extincted objects with extreme ratios of IR to UV/optical luminosity, the IRS is likely to be the only tool to obtain the redshift. Figure 6 shows simulated IRS spectra of an Arp 220-like ULIRG with the low resolution modules at $z = 2$ and with the high resolution modules at $z = 1$. The complete low resolution spectrum would require a few hours of IRS observing, while the high resolution spectrum corresponds to 1000 seconds of integration.

One of the fundamental questions regarding ULIRG's is whether they are powered by starbursts or by AGN. The broad peak at an observed wavelength of 23μm in the low resolution

6 Conclusions

SIRTF's advances over previous IR capabilities will enable dramatic progress to be made on some of today's most pressing questions regarding galaxy formation and evolution. In the broadest terms, *SIRTF* will provide the data needed to understand the connection between the starlight making up the UV/Optical cosmic background and the dust responsible for the CIB.

Surveys with IRAC will enable the generation of field galaxy samples selected on the rest-frame 1.6μm peak out to $z = 4$. Such samples are complementary to those based on the Lyman break, because they are relatively insensitive to dust and to the current star formation rate. These samples will be selected approximately on mass, assuming the local linear scaling of the 1.6μm peak with dynamical mass (i.e., the Tully-Fisher relation) continues to hold at high redshift. By sampling around the rest frame 1.6μm peak, we expect that IRAC will be able to estimate photometric redshifts to 10% for galaxies as bright as L^* to $z > 3$. MIPS observations will allow the study of ULIRG's to $z \sim 3$ and beyond out to 40μm in the rest frame. The resulting spectral energy distributions will define the bolometric luminosities of sources recently found by SCUBA, and establish the degree of overlap between the sub-mm and UV selected populations. IRS observations will provide redshifts for populations too red to measure using ground-based telescopes, and reveal the extent to which AGN vs. starbursts are responsible for the ULIRG component as a function of lookback time.

Finally, with these advances in the capability, it is highly likely that previously unsuspected phenomena will be discovered by *SIRTF*. The opportunity for the astronomical community to make such discoveries is fast approaching: the first proposals for *SIRTF* time will be due in September 2000, with launch a little over a year later.

Acknowledgements. This work was carried out at the Jet Propulsion Laboratory, California Institute of Technology, under a contract with the National Aeronautics and Space Administration. Mark Garcia, Lee Armus, Chris Simpson, and Mark Dickinson provided assistance with the figures, and Giovanni Fazio and Michael Werner provided useful summaries of the *SIRTF* mission and instruments.

References

[1] Barger, A. J., Cowie, L. L., Sanders, D. B., Fulton, E., Taniguchi, Y., Sato, Y., Kawara, K., & Okuda, H. 1998, Nature, 394, 248

[2] Dickinson, M., et al. 1999, ApJ, in press

[3] Dwek, E., et al. 1998, ApJ, 508, 106

[4] Fanson, J., Fazio, G., Houck, J., Kelly, T., Rieke, G., Tenerelli, D., & Whitten, M. 1998, in *Space Telescopes and Instruments V* p. 478, Proc. SPIE 3356

[5] Fazio, G., et al. 1998, Proc. SPIE 3354, 1024

[6] Gardner, J. P., Sharples, R. M., Frenk, C. S., & Carrasco, B. E. 1997, ApJ, 490, L99

[7] Gavazzi, G., Pierini, D., & Boselli, A. 1996, A&A, 312, 397

[8] Hauser, M. G., et al. 1998, ApJ, 508, 25

[9] Lonsdale, C. J. 1999, in *Astrophysics with Infrared Surveys* p. 24, eds Bicay et al., ASP Conference Series 177

[10] Lutz, D., Spoon, H. W. W., Rigopoulou, D., Moorwood, A. F. M., & Genzel, R. 1998, ApJ 505, L103

[11] Heim, G. B., et al. 1998, Proc. SPIE 3356, 985

[12] Hughes, D. H. et al. 1998, Nature, 394, 241

[13] John, T. L. 1988, A&A, 193, 189

[14] Kawara, K., et al. 1998, A&A, 336, L9

[15] Lanzetta, K. M., Yahil, A., & Fernández-Soto, A. 1998, AJ, 116, 1066

[16] Madau, P., Ferguson, H. C., Dickinson, M. E., Giavalisco, M., Steidel, C. C., & Fruchter, A. 1996, MNRAS, 283, 1388

[17] Meurer, G. R., Heckman, T. M., & Calzetti, D. 1999, ApJ, 521, 64

[18] Puget, J. L., et al. 1999, A&A, 345, 29P

[19] Reach, W. T., Puget, J.-L., Lagache, G., Clements, D., & Dole, H. 1999, in *Astrophysics with Infrared Surveys* p. 116, eds Bicay et al., ASP Conference Series 177

[20] Roellig, T. L., et al. 1998, Proc. SPIE 3354, 1192

[21] Sanders, D., & Mirabel, F. 1996, ARA&A, 34, 749

[22] Schmidt, M., Schneider, D. P., & Gunn, J. E. 1995, AJ, 110, 68

[23] Simpson, C., and Eisenhardt, P. 1999, PASP, 111, 691

[24] Steidel, C. C., Giavalisco, M., Pettini, M., Dickinson, M., & Adelberger, K. L. 1996, ApJ, 462, L17

[25] Steidel, C. C., Adelberger, K. L., Giavalisco, M., Dickinson, M., & Pettini, M. 1999, ApJ, 519, 1

[26] Voit, G. M. 1992, ApJ, 399, 495

[27] Wright, E. L., Eisenhardt, P., & Fazio, G. 1994, BAAS, 26, 893